The Effects of Damage on the Energy Absorption of Braided and Non-Crimp Fabric Composite Tubes

K.J. Bottome, N.A. Warrior and D.A. Bailey

School of Mechanical, Materials, Manufacturing Engineering and Management,
University of Nottingham, NG7 2RD, UK

ABSTRACT

The effects of pre-existing damage on the mode of failure and energy absorption characteristics of Non-Crimp Fabric (NCF) and biaxially braided glass/polyester tubular (D/t = 19) sections under axial loading were considered. Damage was induced by controlled out-of-plane impact. Loading rate effects were studied by testing at quasi-static rates and at impact rates of 5m/s. A range of failure modes were exhibited. NCF tubes were seen to splay at static and impact rates – at impact rates a reduction in SEA was recorded. Braided tubes failed in a combination of buckling and splaying at static rates, but under impact all splayed – where a change in failure mode was seen, SEA was increased.

For pre-damaged tubes, a similar effect to that seen previously in continuous filament random mat (CoFRM) glass/polyester tubes was observed, where a threshold size of damage was evident. Below that threshold size the failure mode and SEA were unaffected by the damage, and above that size the tube would fail globally, resulting in a very low SEA. Tubes with high external axial fibre content displayed the greater damage tolerance, other tubes showed a similar damage tolerance to CoFRM. Under dynamic loading the damage tolerance was significantly increased.

1. INTRODUCTION

Composites are ideal for use in lightweight, high-performance crashworthiness applications. They provide a much higher Specific Energy Absorption (SEA) than metals and in optimized structures exhibit a progressive splaying mode of energy absorption, which reduces the cyclic acceleration and deceleration arising from the buckling and folding seen in metallic structures. The effects of geometry, material properties and loading conditions on the SEA are generally well understood and are documented in the literature e.g. [1].

Less understood are the effects of pre-existing damage. Accidental or in-service damage occurs frequently in automotive applications and it is important to understand how damage affects the structure and energy absorption capabilities. A discontinuity can trigger unstable failure in the crushing process, and stress-induced crack growth from the discontinuity can quickly weaken the structure. Recent studies have begun to address this issue [2-4]. In studies [3, 4] the authors observed that in continuous filament random mat glass/polyester composites, a threshold damage size existed, below which the damage had no effect on the mode of failure of the tube, or on the SEA. The tubes in the study failed in 3 distinct and different modes: Failure mode 1 - this was the well-known progressive crushing mode displayed by composites; Failure mode 2 - this was an undesirable global failure, before steady state crushing load was reached, typically a through-thickness crack originated at the damage zone, and propagated circumferentially causing the tube to split and collapse; Failure mode 3 - progressive crushing was established and a local drop-off in load was observed in the vicinity of the damage zone. This drop-off was larger than one that could be attributed to just the reduction in crushing area of the tube, but was smaller than the large decrease seen in failure mode 2. Cracking was seen, but was self-limiting and the load recovered to the steady-state condition after the crush zone passed through the damaged area (see Fig. 1, after [5]).

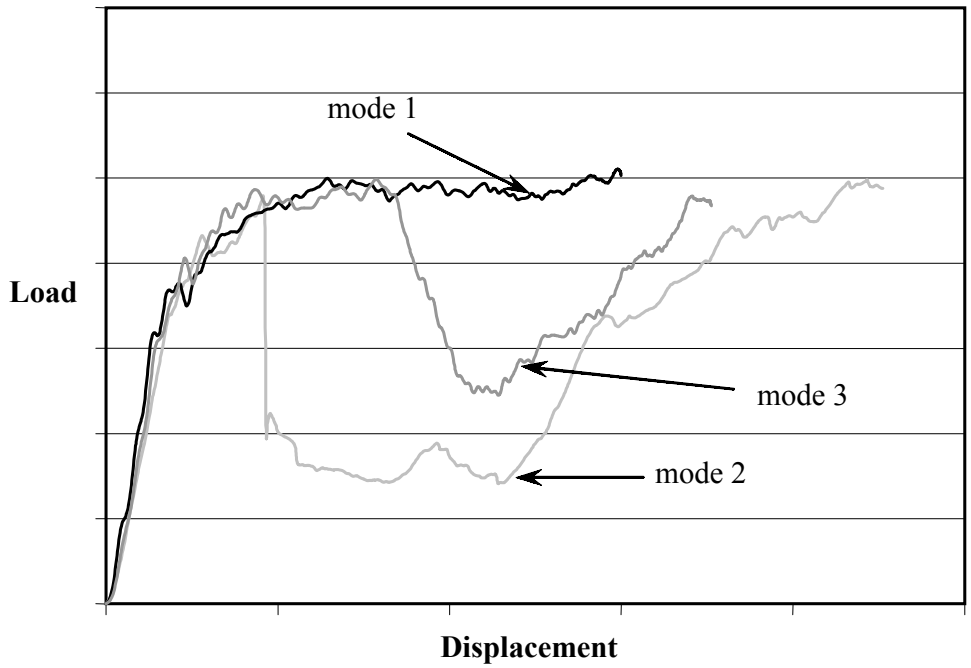

Fig. 1. Load vs displacement curves showing stable and unstable failure, after [5]

The present work aims to expand on the work in [3]-[5] and to investigate the effects of damage tolerance of 6 fibre architectures, based on Non-Crimp Fabrics (NCF) and biaxially braided structures. NCF fabrics offer high in-plane properties via increased directionality and high fibre volume fraction. The fabrics are generally made up of unidirectional layers stitched together, and in this case each ply contains a layer of 0^o tows and a layer of 90^o tows stitched together in the through-thickness direction with polyester yarn. Biaxially braided structures at angles of $^+/_-$ 30^o, 45^o, 60^o were tested (Fig. 2). The braided structures offer improved in-plane properties over the random isotropic material in [3, 4] via increased directionality and high fibre volume fraction, with a reduction in manufacturing costs.

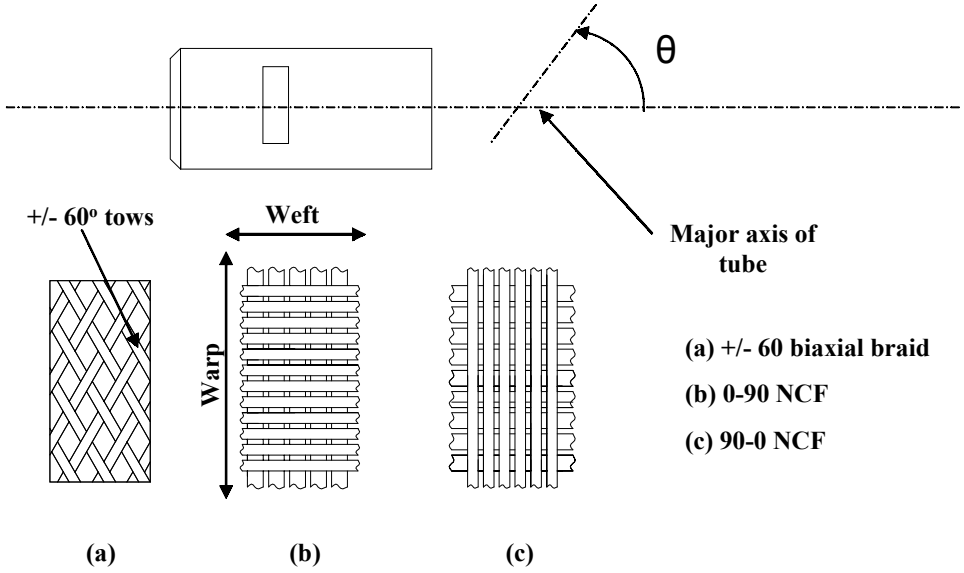

Fig. 2. Representation of fibre architectures.

2. SPECIMEN PREPARATION

Circular glass/polyester tubes of outside diameter 38mm and wall thickness of 2mm (D/t = 19) were produced using a liquid moulding technique in steel tooling to ensure a wall thickness variation of less than 0.1mm.

The NCF reinforcement architecture was an E-glass Non-Crimp Fabric (NCF) (0/90 BTI ELT566 with 283 g/m^2 of fibre in each axis). Each ply consisted of a layer of 0^o tows and a layer of 90^o tows, and as a result of the through-stitching process the tow sizes and spacing in the plies of the NCF were slightly different (see Fig. 2). In this study three orientations of the fabric were used; (a) - with axial fibres on the outside of the outer layer (see Test Reference in Table 2, C1-C5), (b) - Fibres circumferentially on the outer layer (C901-C905) and (c) - with the fibre orientated at 45^o to the major axis of the tube (C451-C455). In the pre-forming process 7% by mass of DSM Resins Neoxil 940 binder was used to allow the fabric to be formed and held. The reinforcement was rolled onto a steel mandrel and consolidated using heat from a hot air gun and pressure from a sprung roller. 3 plies were used to result in a fibre volume fraction of approximately 33%.

The braided architecture was constructed by layers of fibre braided onto a steel mandrel using a single axis, 48 carrier braiding machine. The layers were braided on top of each other until the required diameter was reached. The fibre type was Hybon 2002 600 tex E-glass continuous filament roving. The number of layers and volume fraction data can be seen in Table 1.

Table 1. Tube Construction Data

Fibre architecture	No of layers	Volume Fraction (%)
NCF 0-90	3	33.1
NCF 90-0	3	31.3
NCF +/-45	3	30.3
Braid +/-30	7	33.4
Braid +/-45	5	37.3
Braid +/-60	4	41.3

The resin system used was unaccelerated orthophthalic polyester (Reichold Norpol 420-100: 41-45% styrene content) with 0.5% Akzo-Nobel NL49P accelerator and 1.0% Akzo-Nobel Butanox M50 catalyst.

The tubes were moulded using the Resin Transfer Moulding (RTM) process; resin was injected at 3-4 bar at room temperature for 25 minutes. The mouldings were allowed to cure at room temperature for 24 hours before being extracted. Post curing was carried out at 80^{o}C for 2 hours. The tubes were cut to a length of 80mm using a diamond-cutting saw and a 45^o chamfer was machined onto one end of each specimen, which acted as an initiator to induce stable crush.

Damage was created by an out-of-plane impact, using an impactor tup with a hemispherical end of diameter 12mm (see Fig. 3). The Test Matrix in Table 2 shows the magnitude of the impact energies and the size of the damage zone for the circular tubes tested. Test case C1 was an undamaged tube. In tests C2-C5, damage was created as a result of a controlled impact. Energy levels of 1.5J, 3J, 6J and 9J were delivered on an instrumented falling weight drop tower with a mass of 5.8kg attached. Damage was located at 30mm from the chamfered end along the axis of the tube.

Fig. 3. Damage rig with tup and specimen

Table 2. Test matrix

Fibre Type	Test Reference	Impact Level	Damage Size /mm (axial x hoop)	Quasi-static SEA (kJ/kg) (std. Dev %)	Quasi-static Failure mode	Dynamic SEA (kJ/kg) (std. Dev %)	Dynamic Failure mode
NCF 0-90	**C1**	**None**	**0**	**39.0 (2.7)**	**1**	**32.7 (2.4)**	**1**
NCF 0-90	C2	1.5J	20x15	38.8 (9.8)	1&3	31.1 (3.0)	1
NCF 0-90	C3	3J	32x18	21.0 (16.4)	2	31.7 (7.0)	1
NCF 0-90	C4	6J	45x25	20.3 (11.9)	2	31.7 (0.9)	1
NCF 0-90	C5	9J	50x30	21.4 (13.9)	2	24.1 (15.0)	2&3
NCF 90-0	**C901**	**None**	**0**	**50.4 (1.4)**	**1**	**39.8 (5.8)**	**1**
NCF 90-0	C902	1.5J	22x20	44.7 (34.1)	1&2	44.3 (16.5)	1
NCF 90-0	C903	3J	33x21	46.1 (25.0)	1&2	40.2 (1.0)	1
NCF 90-0	C904	6J	52x28	34.8 (44.5)	2&1	37.5 (8.8)	1&3
NCF 90-0	C905	9J	57x30	39.5 (22.2)	2&1	36.5 (9.1)	3&1
NCF +/-45	**C451**	**None**	**0**	**55.4 (8.0)**	**1**	**29.6 (7.7)**	**1**
NCF +/-45	C452	1.5J	20x15	43.7 (15.8)	1,2,3	30.1 (3.8)	1
NCF +/-45	C453	3J	28x20	28.8 (39.7)	2	27.6 (4.5)	1
NCF +/-45	C454	6J	36x26	19.8 (21.5)	2	28.7 (21.7)	1&2
NCF +/-45	C455	9J	45x28	27.1 (12.0)	2	29.1 (9.4)	2d
Braid +/-30	**CB301**	**None**	**0**	**44.1 (1.1)**	**1**	**30.7 (16.7)**	**1**
Braid +/-30	CB302	1.5J	22x13	37.7 (17.5)	1&2	30.1 (7.8)	1
Braid +/-30	CB303	3J	28x16	36.3 (5.4)	1&2	29.6 (7.1)	1
Braid +/-30	CB304	6J	43x24	31.0 (19.9)	2	31.5 (6.1)	1&2
Braid +/-30	CB305	9J	49x26	38.6 (5.7)	2	31.6 (5.4)	1&2
Braid +/-45	**CB451**	**None**	**0**	**38.8 (3.8)**	**1**	**48.4 (1.4)**	**1**
Braid +/-45	CB452	1.5J	*	32.6 (28.2)	2	46.5 (7.8)	1
Braid +/-45	CB453	3J	*	34.5 (10.0)	2	47.9 (2.0)	1
Braid +/-45	CB454	6J	*	27.5 (13.0)	2	38.9 (8.6)	2
Braid +/-45	CB455	9J	*	28.0 (29.0)	2	39.4 (18.5)	2
Braid +/-60	**CB601**	**None**	**0**	**45.1 (23.0)**	**1&3**	**52.6 (5.1)**	**1**
Braid +/-60	CB602	1.5J	12x16	35.7 (4.8)	2	39.6 (29.9)	1&3
Braid +/-60	CB603	3J	19x22	24.7 (11.5)	2	35.8 (4.6)	2&3
Braid +/-60	CB604	6J	21x27	29.1 (14.0)	2	31.4 (11.8)	2
Braid +/-60	CB605	9J	24x30	27.4 (9.1)	2	32.2 (6.7)	2&3

* No record of damage size

The damage due to impact zone size noted in Table 2 was based on visual inspection of the damage zone and is restricted to the extent of the stress whitening – typically the damage zone shape was ellipsoidal, with the major axis aligned axially and the minor axis circumferential. However the damage zone for the braided $^{+}$/.60 tubes was rectangular in shape with the major axis circumferential and the area of damage was smaller than in all other tubes, see Fig. 4.

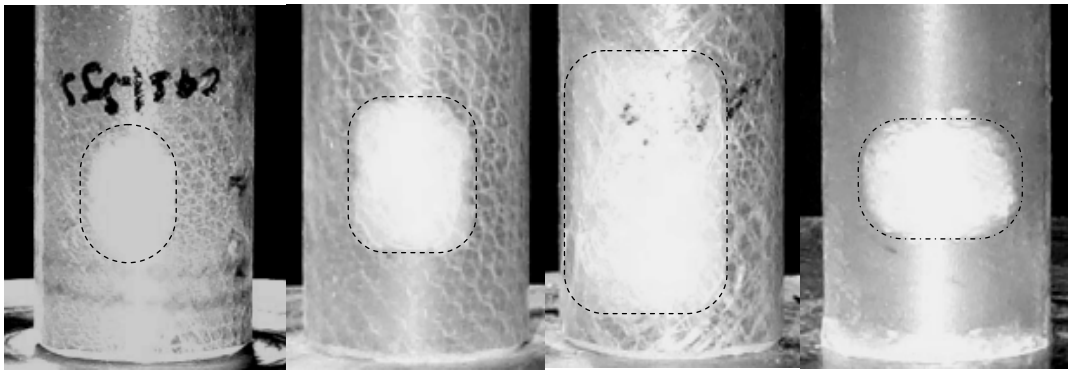

Fig. 4. $^{+}/_{-}$ 45 NCF tube with a) 1.5J, b) 3J, and c) 9J of damage, and d) biaxial $^{+}/_{-}$ 60 tube with 6J of damage

An impact of 1.5J caused a zone of delamination and in-plane matrix damage in all samples, with no visible penetration from the tup. Increasing the energy to 3J caused an increase in the size of the delamination area and evidence of radial and circumferential cracking from the point of impact on the outer and inner surfaces of the tube. Impact damage of 6J increased the damage zone and cracking size and some protrusion on the inner surface of the tube was seen. The impact of 9J caused a further increase in delamination zone with significant circular cracking around the impact zone - there was also visible penetration on the surface of the order of 1mm and a corresponding protrusion on the inner surface of the tube.

3. EXPERIMENTAL METHOD

The specimens were axially crushed at two loading rates: quasi-statically at 5mm/min and dynamically at 5m/s. In both cases samples were crushed onto a steel platen with a ground finish. Quasi-static crush specimens were tested in an electro-mechanical loading frame with 100kN load cell. Dynamic tests were carried out at a nominal impact speed of 5m/s in an instrumented falling weight (drop) tower and impact energy levels were chosen to ensure that there was a minimum of 40 mm of crush in the sample. In the dynamic tests the load data was collecting using a piezoelectric load cell at a sample rate of 40kHz. The mean crush load was calculated by finding the average (or steady-state) crush load after the first 5mm of crush. The first 5 mm of crush was discounted to eliminate the effects from the initiator. Specific Energy Absorption (SEA) values were then calculated by dividing the mean crush load by the mass per unit length of the uncrushed specimens. 3 specimens of each type of sample were tested.

4. RESULTS AND DISCUSSION

The mean SEA results, standard deviations and failure modes are presented in Table 2. The undamaged NCF tubes under static and dynamic testing, failed by progressive crushing in the splaying mode. The 0-90 tubes (C1) split into 5 or more fronds (see Fig. 5(a)). The fronds exhibited significant elastic energy and sprung-back upon removal of the load - the static SEA was 39.0kJ/kg, with a standard deviation over the three test samples of less than 3%. The 90-0 (C901) tubes split into fronds, however, there was visually more resin break-up and fibre damage in the fronds, there was significant curvature and the elastic spring-back seen in the 0-90 tubes was not displayed – consequently the SEA was higher - 50.4kJ/kg with a deviation of 1.4%. The hoop fibres on the external layer of the 90-0 tubes had the effect of constraining the axial fibres, forcing the tube to crush progressively and restricting splaying seen in the 0-90 orientation - this resulted in greater accumulation of intralaminar damage giving a higher SEA. At dynamic rates the resin was seen to pulverize leaving the fibres unsupported and

more able to deform, resulting in a lower SEA (reduced by 16% and 21% for 0-90 and 90-0 respectively). Quasi-statically the NCF $^{+}/_{-}$ 45 tubes showed a splaying mode of crush similar to the 90-0 tubes and absorbed 55.4 kJ/kg (with a deviation of 8.0%), the highest seen for the NCF, but dynamically, the mode of failure is very different. The fibres are unconstrained and splay apart in a spectacular shaped failure absorbing low levels of energy, SEA = 29.6kJ/kg, (Fig. 5(c)).

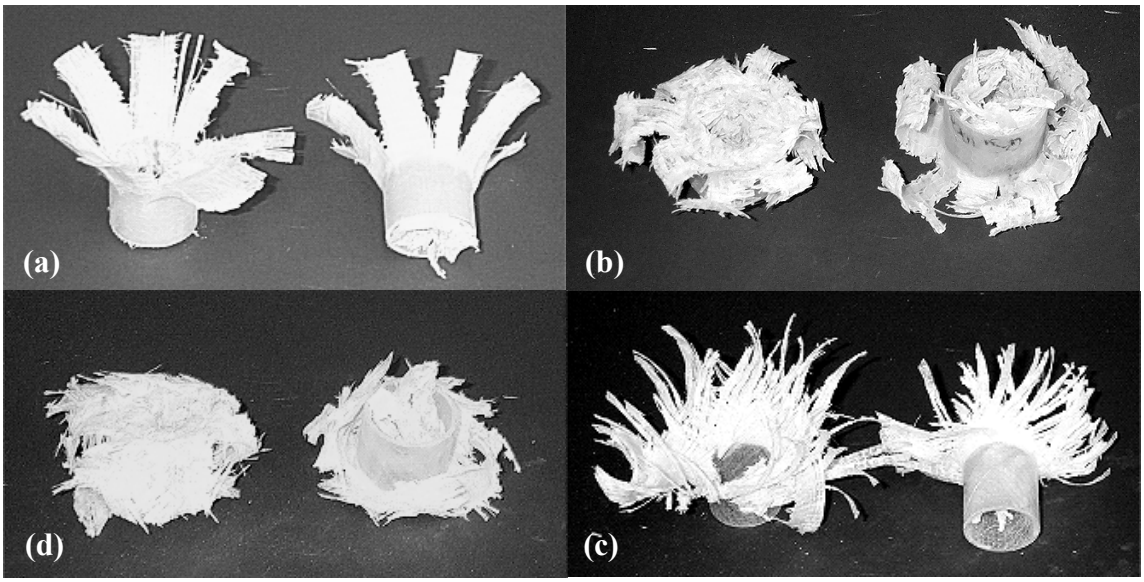

Fig. 5. Modes of failure of NCF tubes, clockwise from top left, (a) 0-90 tube, (b) 90-0 tube, (c) $^{+}/_{-}$ 45 dynamically loaded (d) $^{+}/_{-}$ 45 Quasi-statically loaded

A range of failure modes were seen in the braided tubes. The braided $^{+}/_{-}$30 and $^{+}/_{-}$45 tubes failed progressively under quasi-static loading with a mixture of local folding/buckling and splaying - the outer fronds splayed whilst the inner folded and buckled. The stroke efficiency was reduced in this mode as the buckles stacked up, prohibiting further crush. Splaying dominated the crush zone morphology in the $^{+}/_{-}$60 tubes, where folding was only seen on the inner diameter. For the undamaged braided $^{+}/_{-}$ 30 tube, CB301, the static SEA was 44.1 kJ/kg, with a standard deviation over the three test samples of 1.1%. For $^{+}/_{-}$45 tubes (CB451) the static SEA was 38.8kJ/kg with a deviation of 3.8%, and for $^{+}/_{-}$60 tubes (CB601) static SEA was 45.1kJ/kg with a deviation of 23 % - the high standard deviation indicates the change in crush zone morphology between the three test samples. At quasi-static rates the braid angle had little effect on SEA (see Fig. 7).

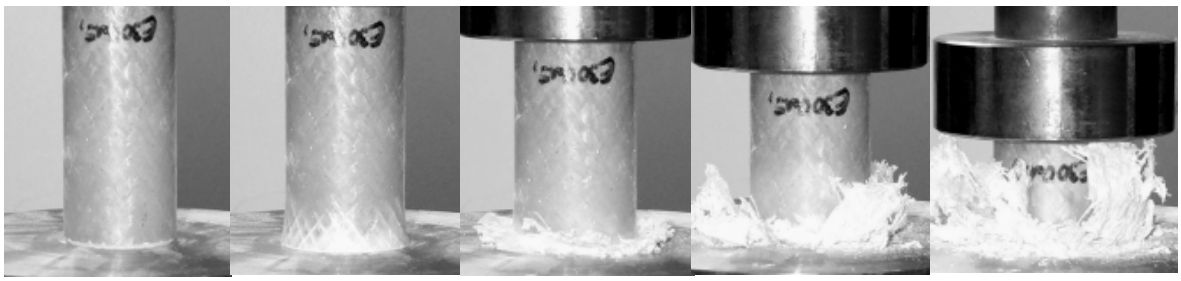

Fig. 6. Sample CB301 showing mode 1 failure (progressive crushing)

Dynamically, the modes of failure changed for the tubes. The $^{+}/_{-}45$ and $^{+}/_{-}60$ tubes splayed in a more progressive manner without buckling and folding. This dynamic splaying mode increased the SEA. The crush zone morphology for $^{+}/_{-}30$ showed more splaying, but with some folding on the inner diameter. Dynamically there was a noticeable difference in SEA for the 3 angles. $^{+}/_{-}30$ had the lowest SEA of 30.7kJ/kg, $^{+}/_{-}45$ was 48.4kJ/kg and $^{+}/_{-}60$ was 52.6kJ/kg (see Fig. 7).

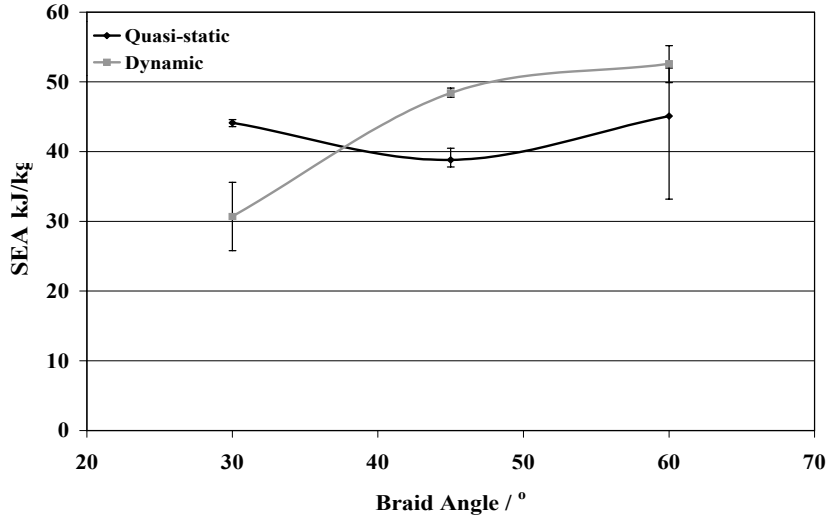

Fig. 7. SEA versus braid angle and Quasi-static and dynamic rates

In the present work, the threshold level is defined as the level at which the first major failure occurs, shown by a reduction in SEA, a change in mode of failure and a corresponding increase in standard deviation to above 10%. When tested with the impact-damage, the 0-90 tubes showed a threshold damage level of 3J quasi-statically and 9J dynamically. Typically, above the threshold level, failure occurred at the edge of the damage zone - a stress-induced crack was formed and quickly propagated along the fibre angles (see Fig. 8). The 90-0 tubes showed a threshold level of 1.5J quasi-statically and 6J dynamically, (although at this level the failure was only local (failure mode 3), and only in one of the three samples). The NCF $^{+}/_{-}45$ tubes had threshold levels of 1.5J quasi-statically and 6J dynamically.

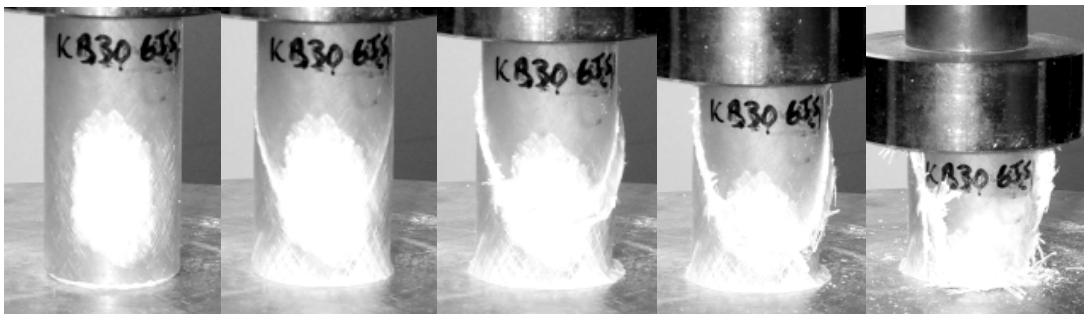

Fig. 8. Sample CB304 showing mode 2 failure, with cracks propagating along fibre angles

Quasi-statically the braided samples all failed with a low threshold level of 1.5J. For the $^{+}/_{-}45$ tubes this represented a decrease in SEA over an undamaged tube of approximately 29%. For the $^{+}/_{-}60$ tube this reduction was 45%. Dynamically the threshold level was significantly increased - the $^{+}/_{-}30$ and $^{+}/_{-}45$ displayed the same threshold value, 6J, although $^{+}/_{-}30$ was more

robust at damage levels above the threshold. Only 1 sample at each level failed globally for the $^{+}/_{-}30$ tubes, whereas all samples fail for the $^{+}/_{-}45$ tubes. At an angle of $^{+}/_{-}60$, the samples showed a threshold damage level of 1.5J, with an SEA of 39.6kJ/kg.

From a comparison of the load displacement curves in Fig. 9 with those in Fig. 1, it can be seen that the behaviour of the NCF tubes is similar to that seen in the CoFRM tubes of the earlier studies [2-4].

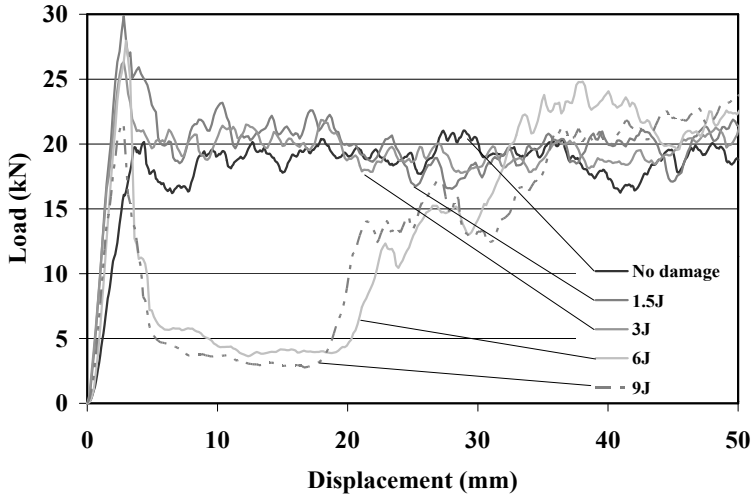

Fig. 9. Load displacement curves for a NCF 90-0 tube

Taking benchmark data from the previous studies, [3-6] the SEAs seen for the NCF and biaxial braid based composites were typically lower than competitor materials (for lightweight automotive body structure applications) - the SEA values for 6061 aluminium tubes of similar geometric ratios (i.e. circular T/d = 19 and square W/d = 15) were both seen to be around 52kJ/kg and the random continuous glass / polyester composite was shown to be up to 75 kJ/kg.

5. CONCLUSIONS

This study has shown that NCF and biaxially braided reinforcements offer relatively low SEA levels - significantly lower than those seen for the CoFRM samples.

The damage caused by out-of-plane impact was seen to have a significant effect on the crush mode. The previously reported threshold damage size effect was seen to apply in NCF at static and impact rates and in braids at impact rates. Statically, the circular NCF 0-90 tubes had a threshold level of 3J - an increase in tolerance over the previously reported CoFRM value of 1.5J [4]. The 90-0 and $^{+}/_{-}45$ NCF tubes showed a static threshold level similar to the CoFRM. Statically, the braided circular tubes had a threshold level of 1.5J, however, the biaxial $^{+}/_{-}30$ tubes appear to show a small improvement in damage tolerance.

At dynamic rates, the damage tolerance of all tubes was increased significantly - in most cases the threshold damage level increased by 2 increments of energy level. The $^{+}/_{-}30$ tubes exhibited the highest tolerance to damage of the braided tubes, indicating that higher axial fibre content limited damage progression around the circumference of the tube, increasing stability.

ACKNOWLEDGEMENTS

The financial support for this programme was provided by the Automotive Composites Consortium (ACC) of the United States Council for Automotive Research (USCAR) and by the University of Nottingham. USCAR is a USA based consortium of Ford Motor Company, DaimlerChrysler, General Motors and the US Department of Energy. Authors acknowledge that this research was supported, in whole or part, by Department of Energy cooperative agreement no. DE-FC05-95OR22363. Such support does not constitute an endorsement by the Department of Energy of the views expressed herein.

References

1. **Hull, D.**, A Unified Approach to Progressive Crushing of Fibre-Reinforced Composite Tubes. Composites Science and Technology, 1991. **44**: p. 376-421.
2. **Karbhari, V.M.**, **et al.**, Post-Impact crush of hybrid braided composite tubes. International Journal of Impact Engineering, 1999. **22**: p. 419-433.
3. **Warrior, N.A.** and **Ribeaux M.**, Effect of Damage on the Energy Absorption of Prismatic Thin-Walled Polymer Composite Structures. Key Engineering Materials, 2002. ISSN: 1013-9826 245
4. **Warrior, N.A.** and **Ribeaux M.**, Effect of Impact Damage on the Specific Energy Absorption of Glass/Polyester. in American Society for Composites 17th Technical Conference. 2002. Purdue University, Indiana, USA.
5. **Warrior, N.A.**, **et al.**, Effects of Fibre Architecture on the Energy Absorption of Damaged Thin-Walled Composite Tubes. in American Society for Composites ASC, 18th Annual Conference. 2003. Florida.
6. **Fernie, R.**, Loading Rate Effects on the Energy Absorption of Lightweight Tubular Crash Structures, PhD thesis. 2002, University of Nottingham: UK.